Intense-field renormalization of cavity-induced spontaneous emission

G.S. Agarwal,* W. Lange, and H. Walther
Sektion Physik der Universität München and Max-Planck-Institut für Quantenoptik, D-85748 Garching, Germany
(Received 18 May 1993)

We examine theoretically the recent experiments of Lange and Walther on the dynamical interaction of Rydberg atoms in a microwave cavity in the presence of a strong driving field. In particular, we study how the intense field renormalizes the cavity-induced spontaneous emission. For this purpose we derive the master equation for the atomic dynamics by adiabatically eliminating the cavity-field variables, while treating the intense driving field nonperturbatively. We present analytical and numerical solutions of the master equation, taking into account the turn on and turn off of the atom-field coupling in the rest frame of the atoms, as well as the velocity distribution of the atomic beam. We obtain good agreement between theoretical results and experiments.

PACS number(s): 42.50.Hz, 32.70.Jz, 42.52.+x

I. INTRODUCTION

It is well known [1–5] that the spontaneous emission characteristics of an atom are modified by the electromagnetic properties of the local environment. In particular, the decay rate Γ_c of an atom in a cavity is given by [1,6,7]

$$\Gamma_c = \Gamma_0 + 2g^2/\kappa, \tag{1.1}$$

where Γ_0 is the spontaneous emission rate into other modes (if available) and $2g^2/\kappa$ is the decay rate into a resonant cavity mode. Here g is the atom-field coupling constant and 2κ is the damping rate of the photon number in the cavity. The rate κ is related to the quality factor Q of the cavity at the resonance frequency ω_c:

$$\kappa = \omega_c/2Q. \tag{1.2}$$

For the case of Rydberg atoms in microwave cavities [6,7], the contribution $2g^2/\kappa$ generally exceeds by far the rate in free space. Several experiments have been reported to measure this cavity-enhanced spontaneous emission [2,8].

Beyond this static effect, recently it has been suggested that spontaneous emission can also be modified dynamically [9]. In this paper we calculate the renormalization of the cavity-induced spontaneous emission by a strong rf field. We consider a beam of two-state Rydberg atoms interacting with a single mode of a microwave cavity driven by an external source. The atoms, which are initially in the upper state, undergo Rabi oscillations while they traverse the resonator. At the same time, the presence of the cavity leads to spontaneous and thermally induced transitions between excited and lower states. The characteristics of these transitions depend on both the Rabi frequency and the detuning of the driving field. The system can be described in terms of the semiclassical dressed states of an atom in a single mode field. In free space and for a resonant driving field one would obtain the Mollow resonance fluorescence triplet [10], which is depicted in Fig. 1. The dashed line in this figure corresponds to the spectral density of the cavity mode. In the experimental situation considered here, the Rabi frequency Ω associated with the strong external field usually exceeds the cavity linewidth κ. Consequently, the fluorescence sidebands fall outside the response spectrum of the cavity mode (cf. Fig. 1), which results in a significant reduction of the cavity-induced decay rate.

In Sec. II we derive the dynamical equations for the atom by eliminating the degrees of freedom associated with the cavity field. As the external field can be arbitrarily strong, we treat it in a nonperturbative way. In Sec. III we obtain approximate dynamical equations for very large Rabi frequencies of the external field and give

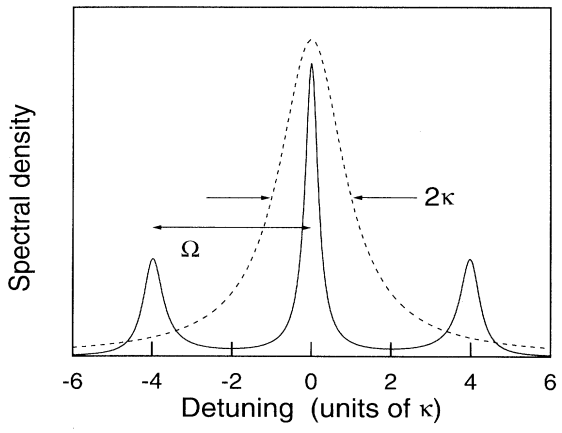

FIG. 1. Mollow triplet of fluorescence in free space (solid curve) and spectral density of a cavity mode (dashed curve). Fluorescence is modified if the Mollow sidebands fall outside the cavity line, which is the experimental situation considered here.

*Permanent address: School of Physics, University of Hyderabad, Hyderabad 500 134, India.

a physical interpretation of these equations. In particular, we examine the cavity-induced transitions among the semiclassical dressed states. The finite temperature of the cavity field is taken into account in all our calculations. In Sec. IV we analyze how the turn on and turn off of the atom-field coupling in the rest frame of the atoms influences the Bloch vector dynamics. Finally, in Sec. V we examine recent experiments with Rydberg atoms in a driven microwave cavity [11] in terms of the theoretical model of the present paper. While our calculations are performed in view of these experiments, it should be mentioned that similar studies in the optical domain have been carried out by Zhu *et al.* [12]. Depending on the detuning of the driving field they observed enhanced or reduced fluorescence when the cavity was tuned to resonance with the sidebands of the Mollow triplet.

II. DYNAMICAL EQUATIONS FOR CAVITY-INDUCED EMISSION IN THE PRESENCE OF AN EXTERNAL FIELD

We consider a two-level atom of frequency ω_0 coupled to a single mode cavity field of frequency ω_c at the finite temperature T. The cavity is driven by an external field of frequency ω_l and amplitude E. The Hamiltonian for this system is

$$H = \hbar\omega_0 S^z + \hbar\omega_c a^\dagger a + \hbar g\left(S^+ a + S^- a^\dagger\right) + \hbar\left(aE^* e^{i\omega_l t} + a^\dagger E e^{-i\omega_l t}\right). \tag{2.1}$$

Here the cavity field is described by the annihilation and creation operators a and $a^\dagger$, while $S^\pm$ and S^z are the spin-$\frac{1}{2}$ angular momentum operators associated with the two-level atom. The cavity has a finite quality factor Q. The cavity relaxation at finite temperature is described by the master equation for the density matrix ρ of the combined atom-field system

$$\begin{aligned}\frac{d\rho}{dt} &= -\frac{i}{\hbar}[H,\rho] + \mathcal{L}\rho\,,\\ \mathcal{L}\rho &= -\kappa(1+\overline{n})\left(a^\dagger a\rho - 2a\rho a^\dagger + \rho a^\dagger a\right)\\ &\quad - \kappa\overline{n}\left(aa^\dagger\rho - 2a^\dagger\rho a + \rho aa^\dagger\right),\end{aligned} \tag{2.2}$$

where $\overline{n}$ is the mean number of thermal photons in the cavity mode.

We will work in a frame rotating at the frequency ω_l of the external field. In this frame the Hamiltonian (2.1) is replaced by

$$H = \hbar\Delta S^z + \hbar\delta a^\dagger a + \hbar g\left(S^+ a + S^- a^\dagger\right) + \hbar\left(aE^* + a^\dagger E\right), \tag{2.3a}$$

where the detunings Δ and δ are defined by

$$\Delta = \omega_0 - \omega_l, \quad \delta = \omega_c - \omega_l. \tag{2.3b}$$

We can now transform to a representation, in which the atom is coupled directly to the classical external field [13], while the quantum cavity field is in the state of thermal equilibrium. We use the unitary displacement operator [14]

$$D(\lambda) = \exp\left(\lambda a^\dagger - \lambda^* a\right), \quad D^\dagger(\lambda)\, a\, D(\lambda) = a + \lambda, \tag{2.4a}$$

where λ is chosen as

$$\lambda = \frac{E}{i\kappa - \delta}. \tag{2.4b}$$

We define the new density matrix ρ' by

$$\rho' = D^\dagger(\lambda)\rho D(\lambda). \tag{2.5}$$

Using Eqs. (2.2), (2.4), and (2.5), we obtain the new master equation

$$\frac{d\rho'}{dt} = -\frac{i}{\hbar}[H',\rho'] + \mathcal{L}\rho', \tag{2.6a}$$

where

$$H' = \hbar\Delta S^z + \hbar\delta a^\dagger a + \hbar g\left(S^+ a + S^- a^\dagger\right) + \frac{\hbar}{2}\left(S^+\Omega + S^-\Omega^*\right). \tag{2.6b}$$

Here, Ω is the Rabi frequency of the classical intracavity driving field given by

$$\Omega = -i\frac{2gE}{\kappa + i\delta} = |\Omega| e^{i\phi}. \tag{2.7}$$

The Lorentzian denominator appearing in (2.7) reflects the fact that for large field-cavity detuning the driving field couples to the cavity less effectively. The detuning dependent phase factor $e^{i\phi}$ may be canceled by redefining the operators $S^+ \to S^+ e^{-i\phi}$ and $a \to ae^{i\phi}$. This transformation does not affect S^z, the quantity being observed in the experiment. Subsequently we will assume that Ω is a real number.

We now write H' as

$$H' = H_0 + V, \quad H_0 = H_a + H_c, \tag{2.8}$$

where H_a and H_c are the unperturbed Hamiltonians for the atom and the cavity field and V is the interaction between the cavity field and the atom:

$$H_a = \hbar\Delta S^z + \frac{\hbar}{2}\Omega\left(S^+ + S^-\right), \tag{2.9a}$$

$$H_c = \hbar\delta a^\dagger a\,, \tag{2.9b}$$

$$V = \hbar g\left(S^+ a + S^- a^\dagger\right). \tag{2.9c}$$

Note that H_0 includes the interaction of the atom with the external field.

When the external field is zero and when the cavity has a low Q factor, so that it is appropriate to think in terms of the cavity-enhanced or -inhibited decay of the atom, one can describe the atomic dynamics by approximately eliminating the cavity field [15]. Let ρ_a be the reduced density matrix for the atomic system alone. For no driving field ($\Omega = 0$), ρ_a is known to be given by [16]

$$\frac{d\rho_a}{dt} = -\frac{ig^2\delta(1+2\overline{n})}{\kappa^2+(\omega_c-\omega_0)^2}\left[S^z,\rho_a\right] - \frac{g^2\kappa(1+\overline{n})}{\kappa^2+(\omega_c-\omega_0)^2}\left(S^+S^-\rho_a - 2S^-\rho_a S^+ + \rho_a S^+S^-\right)$$
$$-\frac{g^2\kappa\overline{n}}{\kappa^2+(\omega_c-\omega_0)^2}\left(S^-S^+\rho_a - 2S^+\rho_a S^- + \rho_a S^-S^+\right). \tag{2.10}$$

Dropping the subscript a from ρ for brevity, the rate equations that follow from Eq. (2.10) are

$$\dot{\rho}_{11} = \frac{-2g^2\kappa}{\kappa^2+(\omega_c-\omega_0)^2}(1+\overline{n})\,\rho_{11} + \frac{2g^2\kappa}{\kappa^2+(\omega_c-\omega_0)^2}\overline{n}\,\rho_{22}\,, \tag{2.11a}$$

$$\dot{\rho}_{22} = -\dot{\rho}_{11}. \tag{2.11b}$$

Thus the excited state decays at a rate

$$\Gamma_{\parallel} = \frac{2g^2\kappa}{\kappa^2+(\omega_c-\omega_0)^2}(1+2\overline{n}), \tag{2.12}$$

which in the limits $\overline{n}\to 0$, $\omega_c\to\omega_0$ reduces to (1.1), the famous result of Purcell [1]. If the cavity is detuned from the atomic resonance, Eq. (2.12) predicts inhibited spontaneous emission [5,8,17,18].

We now return to the question how the atomic dynamics described in Eq. (2.10) is modified by a strong driving field. It should be noted that the derivation of (2.10) assumes that the cavity-field correlation time κ is short compared with the interesting time scales in the problem. The situation changes in the presence of a strong driving field, when $\Omega \gg \kappa$ holds and thus the cavity-field correlation time is large compared to the Rabi flopping time. Such a situation can be handled by working in the basis of semiclassical dressed states $|\pm\rangle$ [19,20]. These states are defined by the eigenvalue equation

$$\left[\hbar\Delta S^z + \frac{\hbar}{2}\Omega\left(S^+ + S^-\right)\right]|\pm\rangle = \pm\frac{\hbar}{2}\overline{\Omega}|\pm\rangle. \tag{2.13}$$

The dressed states are connected to the bare atomic states $|1\rangle$,$|2\rangle$ by the transformation

$$\begin{pmatrix}|+\rangle\\|-\rangle\end{pmatrix} = \begin{pmatrix}\cos\theta & \sin\theta\\ -\sin\theta & \cos\theta\end{pmatrix}\begin{pmatrix}|1\rangle\\|2\rangle\end{pmatrix},$$
$$\begin{pmatrix}|1\rangle\\|2\rangle\end{pmatrix} = \begin{pmatrix}\cos\theta & -\sin\theta\\ \sin\theta & \cos\theta\end{pmatrix}\begin{pmatrix}|+\rangle\\|-\rangle\end{pmatrix}, \tag{2.14}$$

$$\tan\theta = \frac{\overline{\Omega}-\Delta}{\Omega}, \qquad \overline{\Omega} = \sqrt{\Delta^2+\Omega^2}. \tag{2.15}$$

The dipole moment operators $S^{\pm}$ and the population inversion S^z can be written in terms of the operators $R^{\pm}$ and R^z in the new basis as

$$S^{\pm} = 2\cos(\theta)\sin(\theta)\,R^z + \cos^2(\theta)\,R^{\pm} - \sin^2(\theta)\,R^{\mp}, \tag{2.16a}$$

$$S^z = \left(\cos^2\theta - \sin^2\theta\right)R^z - \cos(\theta)\sin(\theta)\left(R^+ + R^-\right), \tag{2.16b}$$

where $R^{\pm}$ and R^z are defined by

$$R^+ = |+\rangle\langle -|, \qquad R^- = |-\rangle\langle +|,$$
$$R^z = \frac{1}{2}\left(|+\rangle\langle +| - |-\rangle\langle -|\right). \tag{2.17}$$

We next introduce the interaction picture by making a canonical transformation using the Hamiltonian

$$H_0 = H_a + H_c = \hbar\Delta S^z + \hbar\delta a^{\dagger}a + \frac{\hbar}{2}\Omega\left(S^+ + S^-\right). \tag{2.18}$$

In this picture the density matrix

$$\tilde{\rho} = e^{iH_0t/\hbar}\,\rho\,e^{-iH_0t/\hbar} \tag{2.19}$$

obeys the master equation

$$\frac{d\tilde{\rho}}{dt} = -\frac{i}{\hbar}\left[\tilde{H}(t),\tilde{\rho}\right] + \mathcal{L}\tilde{\rho}, \tag{2.20}$$

where $\mathcal{L}$ is defined in Eq. (2.2) and we have used

$$\tilde{H}(t) = \hbar g a e^{-i\delta t}\,G(t) + \text{H.c.}\,, \tag{2.21a}$$

$$G(t) = e^{iH_0t/\hbar}\,S^+\,e^{-iH_0t/\hbar}$$
$$= 2\cos(\theta)\sin(\theta)\,R^z + \cos^2(\theta)\,R^+e^{i\overline{\Omega}t} - \sin^2(\theta)\,R^-e^{-i\overline{\Omega}t}. \tag{2.21b}$$

We now eliminate the cavity field adiabatically, keeping the external field to all orders in its strength. By adiabatic elimination we obtain the equation of motion for the reduced density matrix $\tilde{\rho}_a$ of the atom

$$\tilde{\rho}_a = \text{Tr}_c\tilde{\rho}. \tag{2.22}$$

The details of the adiabatic elimination procedure are given in Appendix A. From the resulting master equation for the atom we obtain mean value equations for the dipole moment operator and the inversion in the dressed state basis:

$$
\begin{aligned}
\langle \dot{R}^+ \rangle &= i\overline{\Omega}\langle R^+\rangle - g^2(1+\overline{n})\left\{\frac{\sin^4\theta}{\kappa+i\delta+i\overline{\Omega}}\langle R^+\rangle + \frac{\cos^4\theta}{\kappa-i\delta+i\overline{\Omega}}\langle R^+\rangle\right. \\
&+\frac{2\sin^2(\theta)\cos^2(\theta)\langle R^+\rangle - \sin^3(\theta)\cos\theta}{\kappa+i\delta} + \frac{2\sin^2(\theta)\cos^2(\theta)\langle R^+\rangle - \sin(\theta)\cos^3\theta}{\kappa-i\delta} \\
&+\frac{\sin^2(\theta)\cos^2(\theta)\langle R^-\rangle - 2\sin^3(\theta)\cos(\theta)\left(\frac{1}{2}-\langle R^z\rangle\right)}{\kappa-i\delta-i\overline{\Omega}} \\
&\left.+\frac{\sin^2(\theta)\cos^2(\theta)\langle R^-\rangle - 2\sin(\theta)\cos^3(\theta)\left(\frac{1}{2}+\langle R^z\rangle\right)}{\kappa+i\delta-i\overline{\Omega}}\right\} \\
&-g^2\overline{n}\left\{\frac{\sin^4\theta}{\kappa+i\delta+i\overline{\Omega}}\langle R^+\rangle + \frac{\cos^4\theta}{\kappa-i\delta+i\overline{\Omega}}\langle R^+\rangle\right. \\
&+\frac{2\sin^2(\theta)\cos^2(\theta)\langle R^+\rangle + \sin^3(\theta)\cos\theta}{\kappa+i\delta} + \frac{2\sin^2(\theta)\cos^2(\theta)\langle R^+\rangle + \sin(\theta)\cos^3\theta}{\kappa-i\delta} \\
&+\frac{\sin^2(\theta)\cos^2(\theta)\langle R^-\rangle + 2\sin^3(\theta)\cos(\theta)\left(\frac{1}{2}+\langle R^z\rangle\right)}{\kappa-i\delta-i\overline{\Omega}} \\
&\left.+\frac{\sin^2(\theta)\cos^2(\theta)\langle R^-\rangle + 2\sin(\theta)\cos^3(\theta)\left(\frac{1}{2}-\langle R^z\rangle\right)}{\kappa+i\delta-i\overline{\Omega}}\right\},
\end{aligned}
\tag{2.23a}
$$

$$
\begin{aligned}
\langle \dot{R}^z \rangle &= -g^2(1+\overline{n})\left\{\frac{\cos^4\theta}{\kappa+i\delta-i\overline{\Omega}}\left(\frac{1}{2}+\langle R^z\rangle\right) - \frac{\sin^4\theta}{\kappa+i\delta+i\overline{\Omega}}\left(\frac{1}{2}-\langle R^z\rangle\right)\right. \\
&\left.-\frac{\sin(\theta)\cos^3(\theta)\langle R^+\rangle - \sin^3(\theta)\cos(\theta)\langle R^-\rangle}{\kappa+i\delta}\right\} \\
&-g^2\overline{n}\left\{\frac{\sin^4\theta}{\kappa-i\delta-i\overline{\Omega}}\left(\frac{1}{2}+\langle R^z\rangle\right) - \frac{\cos^4\theta}{\kappa-i\delta+i\overline{\Omega}}\left(\frac{1}{2}-\langle R^z\rangle\right)\right. \\
&\left.-\frac{\sin(\theta)\cos^3(\theta)\langle R^-\rangle - \sin^3(\theta)\cos(\theta)\langle R^+\rangle}{\kappa-i\delta}\right\} + \text{c.c.}
\end{aligned}
\tag{2.23b}
$$

The corresponding modified Bloch equations [9,12] in the original basis are given in Appendix B.

The dynamical equations (2.23) describe the cavity-induced emission in the presence of a driving field. The limit of no external field is obtained by setting θ equal to zero. The resonant structure of the cavity-induced decay terms should be noted. The resonances occur at $\delta = 0$ and $\delta = \pm\overline{\Omega}$, which is reminiscent of the Mollow spectrum in free space [10,21]. In the next section we examine the case of a strong driving field E to understand the physical meaning of the different terms in Eqs. (2.23).

III. INTENSE EXTERNAL FIELD

If the external field is very strong, the dynamical equations (2.23) may be simplified by making a rotating wave approximation. The counterrotating terms oscillate at the frequency $\overline{\Omega}$. Thus we approximate (2.23) by

$$
\langle \dot{R}^+ \rangle = \langle R^+\rangle\left\{i\overline{\Omega} - g^2(1+2\overline{n})\left[\frac{4\kappa\cos^2(\theta)\sin^2\theta}{\kappa^2+\delta^2} + \frac{\cos^4\theta}{\kappa-i\delta+i\overline{\Omega}} + \frac{\sin^4\theta}{\kappa+i\delta+i\overline{\Omega}}\right]\right\}, \tag{3.1a}
$$

$$
\begin{aligned}
\langle \dot{R}^z \rangle &= -2g^2\left(\frac{1}{2}+\langle R^z\rangle\right)\left[(1+\overline{n})\frac{\kappa\cos^4\theta}{\kappa^2+(\delta-\overline{\Omega})^2} + \overline{n}\frac{\kappa\sin^4\theta}{\kappa^2+(\delta+\overline{\Omega})^2}\right] \\
&+2g^2\left(\frac{1}{2}-\langle R^z\rangle\right)\left[(1+\overline{n})\frac{\kappa\sin^4\theta}{\kappa^2+(\delta+\overline{\Omega})^2} + \overline{n}\frac{\kappa\cos^4\theta}{\kappa^2+(\delta-\overline{\Omega})^2}\right].
\end{aligned}
\tag{3.1b}
$$

The decay of the semiclassical states $|\pm\rangle$ is described by the rates $\Gamma_\pm$ given by

$$
\Gamma_+ = 2g^2\left[(1+\overline{n})\frac{\kappa\cos^4\theta}{\kappa^2+(\delta-\overline{\Omega})^2} + \overline{n}\frac{\kappa\sin^4\theta}{\kappa^2+(\delta+\overline{\Omega})^2}\right], \tag{3.2a}
$$

$$
\Gamma_- = 2g^2\left[(1+\overline{n})\frac{\kappa\sin^4\theta}{\kappa^2+(\delta+\overline{\Omega})^2} + \overline{n}\frac{\kappa\cos^4\theta}{\kappa^2+(\delta-\overline{\Omega})^2}\right]. \tag{3.2b}
$$

These rates depend on the strength of the driving field, the cavity-field detuning δ, and the atom-field detuning Δ. The dipole moment in the dressed state basis decays

at the rate $\Gamma_\perp$ given by

$$\Gamma_\perp = g^2(1+2\overline{n})\left[\frac{4\kappa\cos^2(\theta)\sin^2\theta}{\kappa^2+\delta^2}+\frac{\kappa\cos^4\theta}{\kappa^2+(\delta-\overline{\Omega})^2}+\frac{\kappa\sin^4\theta}{\kappa^2+(\delta+\overline{\Omega})^2}\right]. \tag{3.3}$$

The frequency $\tilde{\Omega}$ at which the dipole moment oscillates is shifted from the generalized Rabi frequency $\overline{\Omega}$:

$$\Delta\overline{\Omega} = \tilde{\Omega}-\overline{\Omega} = g^2(1+2\overline{n})\left[\frac{(\delta+\overline{\Omega})\sin^4\theta}{\kappa^2+(\delta+\overline{\Omega})^2}-\frac{(\delta-\overline{\Omega})\cos^4\theta}{\kappa^2+(\delta-\overline{\Omega})^2}\right]. \tag{3.4}$$

Using the above definitions, the Bloch equations (3.1) for an intense driving field read

$$\langle\dot{R}^+\rangle = \langle R^+\rangle\left(i\tilde{\Omega}-\Gamma_\perp\right), \tag{3.5a}$$

$$\langle\dot{R}^z\rangle = -\langle R^z\rangle(\Gamma_+ + \Gamma_-) - \frac{1}{2}(\Gamma_+ - \Gamma_-). \tag{3.5b}$$

The solution is easily found to be

$$\langle R^+(t)\rangle = \langle R^+(0)\rangle e^{(i\tilde{\Omega}-\Gamma_\perp)t}, \tag{3.6a}$$

$$\langle R^z(t)\rangle = -\frac{1}{2}\frac{\Gamma_+-\Gamma_-}{\Gamma_++\Gamma_-} + \left[\langle R^z(0)\rangle + \frac{1}{2}\frac{\Gamma_+-\Gamma_-}{\Gamma_++\Gamma_-}\right]e^{-(\Gamma_++\Gamma_-)t}. \tag{3.6b}$$

The dressed state population inversion $\frac{1}{2}-\langle R^z\rangle$ decays at the rate

$$\Gamma_\parallel = \Gamma_+ + \Gamma_- = 2g^2(1+2\overline{n})\left[\frac{\kappa\cos^4\theta}{\kappa^2+(\delta-\overline{\Omega})^2}+\frac{\kappa\sin^4\theta}{\kappa^2+(\delta+\overline{\Omega})^2}\right]. \tag{3.7}$$

Using the dependence (2.7) of the intracavity Rabi frequency Ω on the detuning δ, we can calculate the decay rates $\Gamma_\parallel, \Gamma_\perp$ and the dynamic shift of the Rabi frequency $\Delta\overline{\Omega}$ as a function of the driving field detuning. Figure 2 shows the result for the cavity in resonance with the atomic transition ($\Delta = \delta$). We first observe that for large positive or negative detuning the three quantities assume their zero-field values, as it must be, because far from the cavity resonance the external field does not couple to the intracavity field owing to Eq. (2.7). If the driving field Ω is tuned closer to resonance, its influence on the system dynamics grows, resulting in a decrease of the decay rates $\Gamma_\parallel$ and $\Gamma_\perp$ and an increase of the Rabi frequency $\tilde{\Omega}$. At a critical detuning

$$\Delta_c = \sqrt[3]{\frac{2g^2E^2}{\kappa}}, \tag{3.8}$$

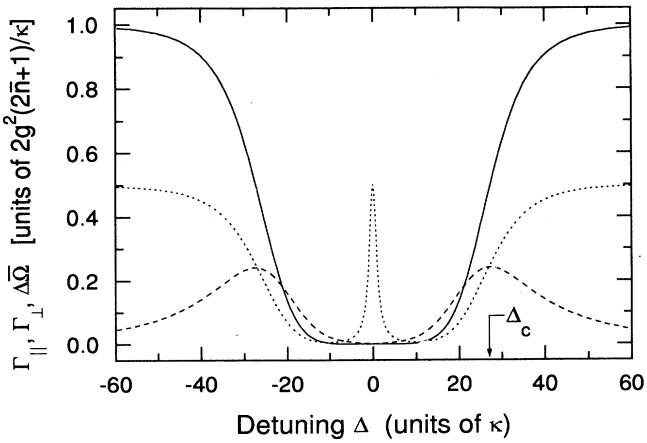

FIG. 2. Scaled decay rates $\Gamma_\parallel$ (solid curve), $\Gamma_\perp$ (dotted curve), and shift of the generalized Rabi frequency $\Delta\overline{\Omega}$ (dashed curve) as a function of the atom-field detuning in the strong field limit. The cavity is in resonance with the atomic transition. The Rabi frequency of the driving field at zero detuning is $2gE/\kappa = 200\kappa$.

the decay rates have dropped to half their zero-field values. At the same time the shift of the generalized Rabi frequency reaches its maximum. Tuning the field to resonance with atoms and cavity, we obtain a decay rate $\Gamma_\parallel$ that is reduced by a factor of $(\kappa/\overline{\Omega})^2$ compared to the zero-field result. Therefore, $\Gamma_\parallel$ can be made arbitrarily small by increasing the input field E. This result shows that atomic decay can be completely suppressed by a strong driving field, if the atomic Bloch vector is aligned with the dressed frame z axis, that is, if the atom is in a dressed state. In the case of a nonzero dressed state polarization, i.e., for a superposition of dressed states, the decay of the $\langle R^\pm\rangle$ components has to be taken into account. As long as the detuning of the driving field is larger than the cavity linewidth κ, the decay rate $\Gamma_\perp$ is suppressed by the same factor as $\Gamma_\parallel$. For detunings $\Delta = \delta \lesssim \kappa$, however, the decay rate increases again, reaching its zero-field value at $\Delta = \delta \approx 0$. This is due to the term peaked at $\delta = 0$ in Eq. (3.3). Consequently, at zero detuning spontaneous emission cannot be completely suppressed if there is a finite dressed state polarization.

In contrast to the optical domain, in the Rydberg atom experiment we consider here, the cavity is closed on all sides, apart from small holes for the atomic beam injection and coupling of the external microwave field. This has two notable consequences. First, the atom does not couple to modes of the continuum. Therefore, suppression of decay into the cavity mode means that the atom does not decay at all, as there are no other decay channels available. At the same time, the observation of atomic fluorescence in the cavity is ruled out. The only source of information on the atom-cavity interaction is the state of the atoms leaving the cavity. Consequently, $\Gamma_\parallel$ cannot be measured directly, but has to be inferred, for example, from the lower level population $P_2 = 1/2 - \langle S^z\rangle$ of the

atoms leaving the cavity.

It should be noted that the experiment we describe involves a transient situation, as the transit time T is of the same order of magnitude as the photon lifetime $(2\kappa)^{-1}$ in the cavity.

As was shown above, the suppression of atomic decay depends on the orientation of the Bloch vector in the dressed frame. Complete suppression can only be achieved if it is oriented along the z axis. In the next section we will show that, if the atoms are prepared outside the cavity, the alignment of the Bloch vector and hence the modification of spontaneous emission is determined by the diabatic or adiabatic change of the atom-cavity coupling when the atoms enter the cavity.

IV. INFLUENCE OF TIME-DEPENDENT COUPLING ON THE BLOCH VECTOR DYNAMICS

In the preceding sections we have implicitly assumed that the coupling g of the atoms to the cavity field is a constant. Experimentally, however, the atoms are prepared outside the cavity, where they do not couple to the cavity field at all. Likewise, the detection of the atoms is performed after they have left the cavity. Consequently, in their rest frame the atoms experience a time dependent coupling to both the cavity field and the driving field. The exact shape of $g(t)$ is determined by the cavity mode. It must be taken into account in a realistic model. In the experiment we describe, inside the cavity the coupling has a constant value g_0 along the cavity axis. Due to leakage of the cavity field, at the entrance and exit holes the coupling decreases exponentially on a scale α^{-1}, where α is the rf attenuation constant of the holes. While entering or leaving the cavity, the atoms are subject to a field envelope changing on a time scale τ defined by

$$\tau = \frac{\pi}{\alpha v} = \frac{\pi T}{\alpha L}, \tag{4.1}$$

where v is the atomic velocity, L the length of the cavity, and T the transit time.

One consequence of the gradual turn on and turn off of the coupling is that the atoms pass a region, where cavity-enhanced spontaneous emission already takes place, while the coupling to the driving field is yet too weak to completely suppress the decay dynamically. This is demonstrated in Fig. 3, where we show the decay rate $\Gamma_{\|}$ as a function of the coupling g for different values of the driving field amplitude E. The resulting peak in the decay rate affects the atoms only for a small fraction of the total transit time and thus contributes little to the final lower level occupation. Therefore, in this section we will neglect atomic decay during the turn on and turn off phases.

A much more important aspect is that, according to Eq. (2.7), the time dependence of the coupling $g(t)$ also determines the rate of change of the intracavity Rabi frequency $\Omega(t)$. The rise time τ of the Rabi frequency, on the other hand, determines the atomic dynamics during

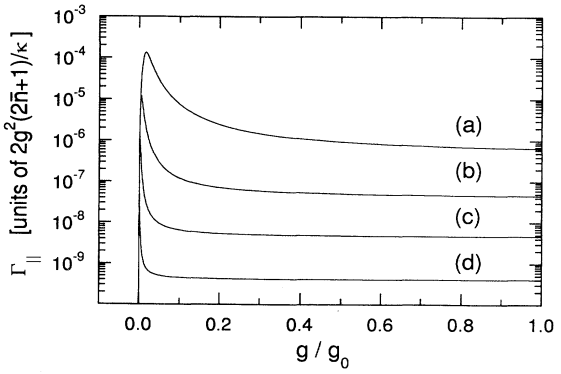

FIG. 3. Scaled decay rate $\Gamma_{\|}$ as a function of the coupling g. The detuning is $\Delta = 75\kappa$, the Rabi frequencies are (a) $2g_0E/\kappa = 30\kappa$, (b) $2g_0E/\kappa = 100\kappa$, (c) $2g_0E/\kappa = 300\kappa$, and (d) $2g_0E/\kappa = 1000\kappa$. The maximum is due to the balance between cavity-enhancement and dynamic suppression of spontaneous emission.

the turn on of the coupling [22], the important quantity being the product $\tau\Delta$. Thus the superposition of the dressed states $|+\rangle$, $|-\rangle$, in which the atom is found inside the cavity, depends critically on the mode function $g(t)$. Once the atomic state at the end of the entrance phase is known, it can be used as initial condition for Eqs. (3.6), which yield the solutions $\langle R^+\rangle$ and $\langle R^z\rangle$ at the cavity exit. These have to be propagated through the turn off phase to obtain as the final result the lower level population at the detector.

The situation is particularly simple if the detuning Δ is large compared to the inverse rise time τ^{-1} of the coupling in the rest frame of the atoms. In this case the transition from zero to the full coupling is adiabatic and the atoms are always in an eigenstate of the Hamiltonian H_a. For positive Δ, for example, an atom prepared in state $|1\rangle$ will end up in the dressed state $|+\rangle$, while $|2\rangle$ is transformed into $|-\rangle$. The reverse process occurs at the cavity exit. Therefore, the atoms would leave the cavity in the same state they entered, if they would not undergo spontaneous and thermally induced transitions inside the cavity.

In Fig. 4 we show the time development of the z component of the Bloch vector in the bare state basis for three values E of the driving field. It was obtained by numerically integrating Eqs. (B3) in Appendix B. For weak driving fields the atomic inversion decays exponentially and the atoms leave the cavity in thermal equilibrium [trace (a)]. Increasing the external field E to values much larger than κ strongly suppresses decay inside the cavity. Nearly total inversion is recovered upon exit [trace (c)]. The probability for lower state detection of atoms leaving the cavity can be calculated analytically from solution (3.6b):

$$P_2 = \rho_{22} = \rho_{--} = \frac{1}{2} - \langle R^z\rangle = \frac{\Gamma_+}{\Gamma_{\|}} - \left[\langle R^z(0)\rangle + \frac{1}{2}\frac{\Gamma_+ - \Gamma_-}{\Gamma_{\|}}\right] e^{-\Gamma_{\|}T}. \tag{4.2}$$

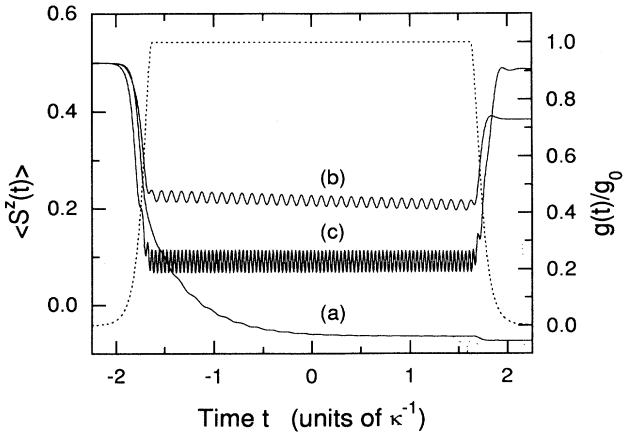

FIG. 4. Time development of the z component of the Bloch vector in the bare state atomic basis. The dotted line is the cavity mode envelope (i.e., the relative size of the coupling g). For the edges a hyperbolic secant function of width $\tau = 0.2\kappa^{-1}$ was chosen. The transit time is $T = 2.6\kappa^{-1}$, the coupling inside the cavity is $g_0 = 2.5\kappa$, and the thermal photon number is $\overline{n} = 2.9$. The three traces correspond to (a) $E = 150\kappa$, (b) $E = 500\kappa$, and (c) $E = 1500\kappa$. The detuning $\Delta = 38\kappa$ is such that the atom passes the cavity field adiabatically. Trace (c) shows almost complete suppression of decay, as the atom leaves the cavity in roughly the same state it entered.

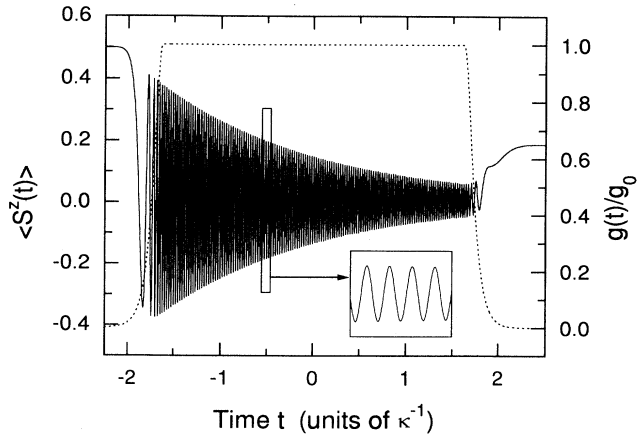

FIG. 5. Time development of the z component of the Bloch vector in the bare state atomic basis. The detuning is $\Delta = 7.5\kappa$, corresponding to atoms entering the cavity field nonadiabatically. This leads to strong Rabi flopping as well as a finite decay rate. The field strength is $E = 500\kappa$, the other parameters are the same as in Fig. 4.

The dynamics is more complicated if the external field is close to resonance ($|\tau\Delta| < 1$). In this case the fast turn on of the driving field leads to a nonadiabatic change of the Bloch vector, putting the atom in a superposition of the two dressed states, i.e., in a state with nonzero dipole moment. For $\Delta = 0$, for example, the resulting atomic state is $(|+\rangle + e^{i\varphi}|-\rangle)/\sqrt{2}$. The presence of a finite dressed state dipole moment distinguishes the Bloch vector motion from that in the adiabatic case. According to solution (3.6a), the dipole moment undergoes Rabi oscillations and, at the same time, decays at the rate $\Gamma_\perp$, which has a finite value around zero detuning (cf. Fig. 2). Figure 5 illustrates the decay and Rabi flopping of the Bloch vector in the nonadiabatic case. If the Rabi oscillations are not completely damped during transit, atoms leaving the cavity retain a dressed state dipole moment. This makes the final bare state atomic inversion dependent on the Rabi frequency, the transit time, and the decay rate $\Gamma_\perp$. In addition, transitions between atomic levels are induced by the nonadiabatic nature of the cavity field turn off. This contribution to the change of atomic population is independent of cavity-induced effects.

Generally, in the case of nonadiabatic passage there is no simple expression for the atomic dynamics generated by the time dependent coupling and hence for the initial condition in Eqs. (3.6). However, for one particular shape of the mode envelope $g(t)$, an analytical solution exists [23,24]. In Appendix C we apply this solution to derive an expression for the inversion $\langle S_z \rangle$ of the atoms leaving the cavity. Here we would like to present only graphically the results of this calculation. In Fig. 6 we show the probability for detecting an atom leaving the cavity in the lower state as a function of the atom-field detuning. For large Δ, the solution coincides with Eq. (4.2). There is an extended region, where almost no transitions to the lower state occur, due to the dynamic suppression of spontaneous emission. For smaller Δ the transition rate increases again and oscillations appear, which are due to the nonadiabatic effects described above. The oscillation frequency as a function of detuning is determined by Eqs. (2.15) and (3.4) for the shifted generalized Rabi frequency.

In the experiment, these fast oscillations will be washed out, as even in a velocity selected atomic beam the distribution of transit times has a width much larger than the inverse Rabi frequencies considered here. Averaging over a symmetric velocity distribution leads to a smooth

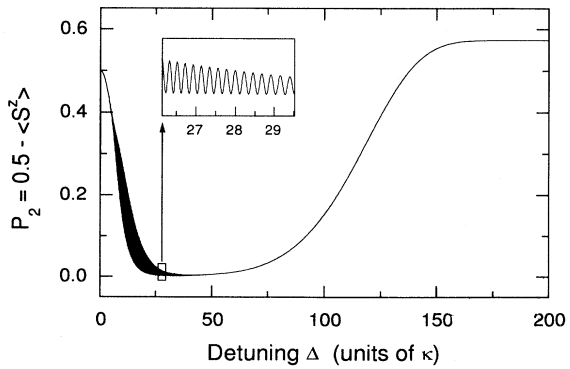

FIG. 6. Lower level population of a monokinetic atomic beam at the cavity exit as a function of the atom-field detuning. The parameters used are $E = 1500\kappa$, $g_0 = 2.5\kappa$, $\kappa\tau = 0.2$, $\kappa T = 2.6$, and $\overline{n} = 2.9$.

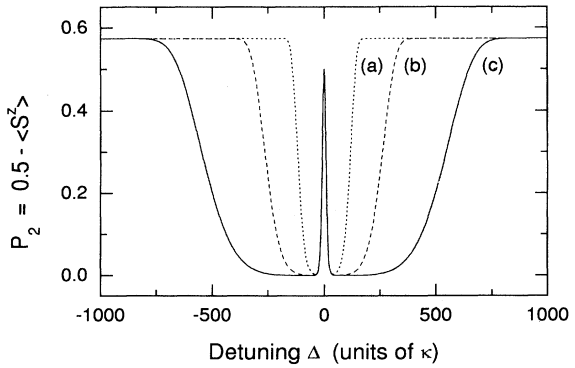

FIG. 7. Lower level population for a beam with a narrow symmetrical velocity distribution. The field strengths are (a) $E = 1500\kappa$, (b) $E = 5000\kappa$, and (c) $E = 15\,000\kappa$. The other parameters are the same as in Fig. 6.

curve for the lower level detection probability, as is shown in Fig. 7. The three traces correspond to different amplitudes E of the driving field.

From Eqs. (4.2) and (3.7) an expression for the width w of the range where suppression occurs can be obtained for $E \gg \kappa$:

$$w = \left(\sqrt{\frac{2\ln 2}{1+2\bar{n}}} C_1 \frac{16E^2}{T} \right)^{1/3}. \tag{4.3}$$

Here $C_1 = g_0^2 T/4\kappa$ is the one-atom bistability parameter.

V. COMPARISON WITH EXPERIMENTS ON CAVITY-INDUCED EMISSION IN THE PRESENCE OF AN EXTERNAL FIELD

In this section we apply our results to interpret recent experiments [11] at the Max-Planck-Institut für Quantenoptik in Garching. The experiments are performed with a thermal beam of Rydberg atoms traversing a superconducting resonant microwave cavity driven by an external source.

The theory we have presented in Sec. IV has to be refined in some respects, to take into account the specific experimental situation.

First, in the experiment a thermal atomic beam is employed. The distribution of transit times $P(T)$ is given by

$$P(T)dT = \frac{4}{\sqrt{\pi}T_0} \left(\frac{T_0}{T} \right)^4 e^{-\left(\frac{T_0}{T}\right)^2} dT, \tag{5.1}$$

T_0 being the transit time corresponding to the most probable velocity in the beam. As $P(T)$ is not symmetric about T_0, the results will slightly differ from those presented in Fig. 7. The experimental value for T_0 is about $2.6\kappa^{-1}$.

The second aspect is the time dependence of the coupling $g(t)$ in the rest frame of the atoms. A better approximation to the experimental situation than (C1), used for the analytical calculation, is given by

$$g(t) = \frac{g_0}{2} \left\{ 1 - \tanh \left[\frac{\pi}{\tau} \left(|t| - \frac{T+\tau}{2} \right) \right] \right\}. \tag{5.2}$$

The modified shape of the leading and trailing edge of the coupling changes the atomic dynamics upon entrance and exit and hence could lead to different decay characteristics. In the experiment the rise time τ is $0.077T$.

Finally, decay during turn on and turn off of the coupling, which was neglected in Sec. IV, has been added in the numerical calculations.

Taking into account the modified mode shape as well as decay, we numerically integrated Eqs. (B3) in Appendix B for fixed transit times T. Subsequently we averaged over the velocity distribution (5.1). The result is shown in Fig. 8, together with the analytical solution obtained above. The peak at zero detuning is slightly broader, while the width of the region where suppression of decay occurs shrinks. These small quantitative deviations are mainly due to the modified edges of the coupling. As the qualitative behavior is the same in both cases, the interpretation of the phenomena we have presented in Sec. IV still applies.

In the experiment the count rate of atoms leaving the cavity in the lower state was recorded as a function of the atom-field detuning. In Fig. 9 we present the measured data, together with the corresponding theoretical result, which is in quite good agreement. Both curves feature the nearly complete suppression of transitions over a tuning range of the driving field of roughly $\pm 500\kappa$. The theoretically predicted sharp central peak is also observed, indicating the presence of a finite dressed state polarization due to nonadiabatic effects. The fraction of lower level atoms for large Δ is equal to the value in the absence of the external field, $(1+\bar{n})/(1+2\bar{n})$, which can be determined from the stationary solution of Eqs. (2.11a).

An important aspect in Rydberg atom experiments, which has not been addressed yet, is inhomogeneous

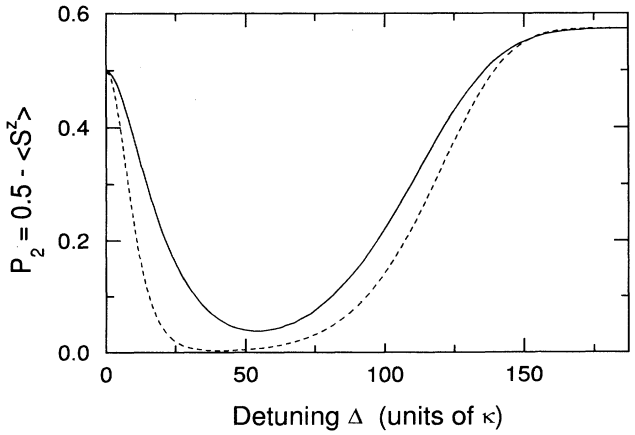

FIG. 8. Lower level population for $E = 1500\kappa$ and the parameters used in Fig. 6. The solid curve was obtained by numerically integrating the modified Bloch equations. The dotted curve represents the analytical result presented in Appendix C.

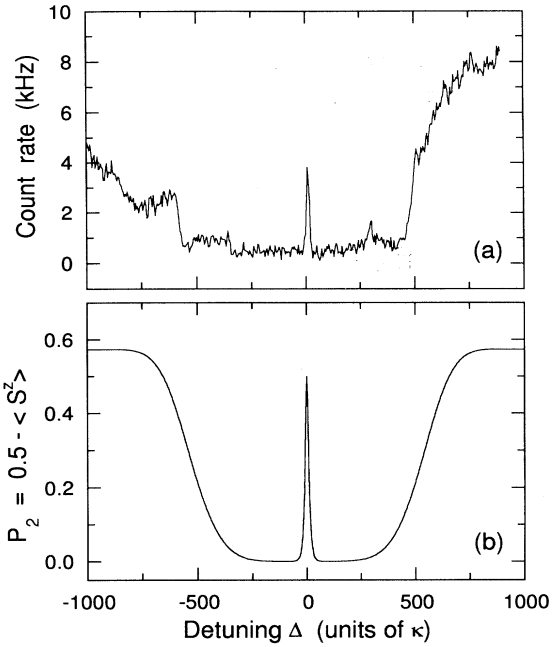

FIG. 9. (a) Experimental trace of the lower level population at $E = 15\,000\kappa$. $\kappa/2\pi = 6.7$ kHz, $g_0 = 2.5\kappa$, $\kappa T_0 = 2.6$, $T/\tau = 13$, and $\overline{n} = 2.9$. The atomic beam has a thermal velocity distribution. (b) Corresponding theoretical curve.

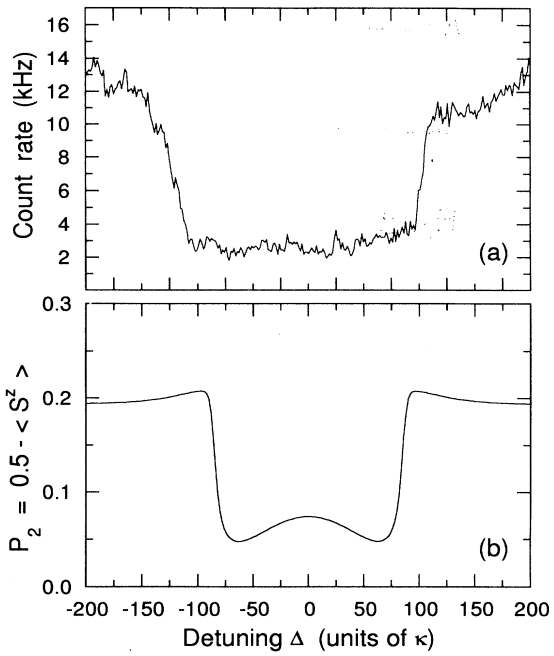

FIG. 10. (a) Experimental trace of the lower level population at $E = 1500\kappa$ in the presence of strong inhomogeneous broadening. Otherwise the parameters are the same as in Fig. 9. (b) Theoretical curve, assuming an inhomogeneous linewidth of 75κ. The central peak vanishes, while the edges of the suppression profile get steeper.

broadening of the atomic line. It is mainly due to random Stark shifts in electric stray fields that are caused by atoms deposited on the cavity wall. This process occurs irreversibly in the course of an experimental run and periodical cleaning of the cavity is necessary to obtain reproducible results. Figure 10(a) shows a spectrum recorded with a contaminated resonator, which had been in use for an extended period. Suppression of decay is still present even under conditions of strong inhomogeneous broadening, but the central peak observed in Fig. 9(a) does not show up. We have modeled this experimental situation by averaging $\langle S^z \rangle$ over a Gaussian distribution of atomic transition frequencies. For simplicity we have used the analytical expression (C16) for $\langle S^z \rangle$, which can be readily evaluated. The result is shown in Fig. 10(b). The central peak, indeed, vanishes. At the same time the edges of the suppression range acquire a substantially steeper slope, again in agreement with the experimental observation.

We have also investigated the threshold for the onset of dynamic suppression of decay by monitoring the lower level count rate as a function of the input field E [Fig. 11(a)]. Taking into account inhomogeneous broadening we can reproduce the shape of the threshold [Fig. 11(b)], obtaining a threshold amplitude of $E \approx 10\kappa$. This corresponds to about 100 photons in the cavity mode.

Finally, we have put our theory to another test by comparing expression (4.3) for the width w of the suppression range with the experimental data. The predicted cube root behavior of w as a function of the injected power is in perfect agreement with observations, at least in the

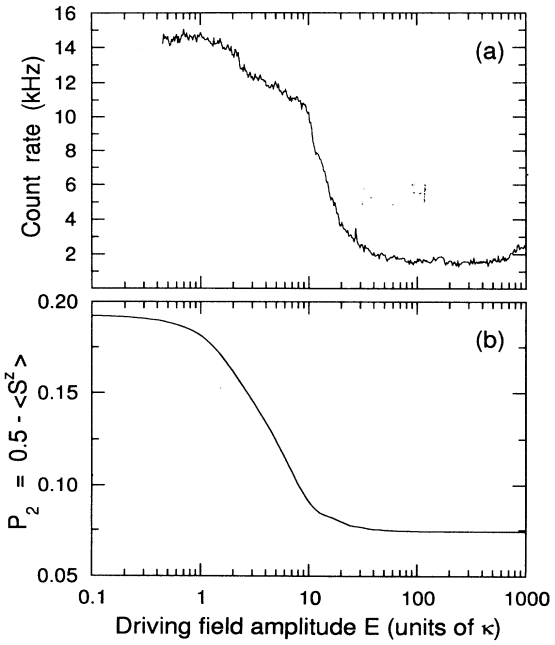

FIG. 11. (a) Experimental curve of the lower level population with inhomogeneous broadening as a function of the input field amplitude E, showing the threshold for the suppression of emission. Field, atoms, and cavity are on resonance. (b) Theoretical curve for an inhomogeneous linewidth of 75κ.

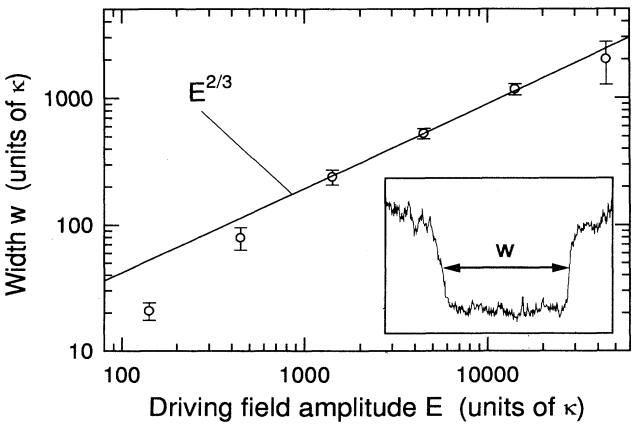

FIG. 12. Measured width of the range where dynamic suppression is observed. The solid line represents the theoretical result in the strong field case ($2g_0E/\kappa \gg \kappa$).

strong field limit assumed in the derivation of (4.3). This is shown in Fig. 12. Numerical calculations confirm that at smaller intensities the slope of w increases.

VI. SUMMARY

In conclusion, we have shown how the atomic dynamics in a microwave cavity driven by a strong external field can be formulated to study cavity-induced atomic decay and its modification by the intense field. We have applied the theory to interpret the experimental results of Lange and Walther with Rydberg atoms in a superconducting cavity. The experiments differ from similar studies in the optical domain in that the atoms couple only to a single cavity mode and not to the continuum. The observable that is monitored is the lower level population of atoms leaving the cavity. Over a large tuning range of the driving field, there is almost complete suppression of the lower level count rate, if the driving field is strong enough. In our model this is explained by the dynamic renormalization of the atomic decay rate. We obtain good quantitative agreement between theory and observations, taking into account the inhomogeneous broadening of the atomic transition.

An important observation is that in the experiment, transitions are not suppressed for detunings of the driving field that are small compared to the inverse rise time of the field. The phenomenon can be traced back to the generation of nonzero dressed state polarization when the atoms enter the cavity field non-adiabatically.

APPENDIX A: ADIABATIC ELIMINATION OF THE CAVITY FIELD

In this section we discuss the adiabatic elimination of the cavity field from the density matrix equation (2.20) which we rewrite as

$$\frac{d\tilde{\rho}}{dt} = -\frac{i}{\hbar}\left[\tilde{H}(t),\tilde{\rho}\right] + \mathcal{L}\tilde{\rho}, \tag{A1}$$

where $\mathcal{L}$ is the field relaxation operator defined in Eq. (2.2). We make another transformation to σ defined by

$$\sigma(t) = e^{-\mathcal{L}t}\tilde{\rho}(t). \tag{A2}$$

On using (2.21) and (A2), Eq. (A1) reduces to

$$\frac{d\sigma(t)}{dt} = -\frac{i}{\hbar}\left[H_\sigma(t),\sigma(t)\right], \tag{A3}$$

where

$$\begin{aligned} H_\sigma(t) &= \hbar g\, a(t)\, e^{-i\delta t}\Big[2\cos(\theta)\,\sin(\theta)\,R^z \\ &\quad + \cos^2(\theta)\,R^+\,e^{i\bar{\Omega}t} \\ &\quad - \sin^2(\theta), R^-\,e^{-i\bar{\Omega}t}\Big] + \text{H.c.} \\ &= \hbar g\, a(t)\, e^{-i\delta t}\, G(t) + \text{H.c.}\,, \\ a(t) &= e^{-\mathcal{L}t}\, a\, e^{+\mathcal{L}t}. \end{aligned} \tag{A4}$$

Note that Eq. (A3) involves only the cavity-atom interaction. Assuming that the interaction g is weak (the precise condition will be given at the end of this section), we can do a second order perturbation calculation with respect to g. Note further that

$$\tilde{\rho}_a(t) = \mathrm{Tr}_c\,\tilde{\rho}(t) = \mathrm{Tr}_c\,\sigma(t). \tag{A5}$$

Using standard projection operator techniques to eliminate the cavity field variables, Eq. (A3) leads to

$$\frac{d\tilde{\rho}_a(t)}{dt} = -\int_0^\infty d\tau\,\mathrm{Tr}_c[H_\sigma(t),\,[H_\sigma(t-\tau),\rho_c(0)\tilde{\rho}_a(t)]], \tag{A6}$$

where $\rho_c(0)$ is the density matrix of the cavity field in the absence of the atom and the external field. The Markov approximation is now justified as in the picture in which (A3) is derived, the dynamics is entirely due to the cavity field. On substituting (A4) in (A6), we get terms involving correlation functions of the cavity field. These correlation functions can be obtained from the master equation describing relaxation at finite temperatures. They are known to be

$$\begin{aligned} \mathrm{Tr}_c\,a(t)a^\dagger(t-\tau)\,\rho_c &\equiv \langle a(t)a^\dagger(t-\tau)\rangle = (\bar{n}+1)\,e^{-\kappa\tau}\,, \\ \mathrm{Tr}_c\,a^\dagger(t)a(t-\tau)\,\rho_c &\equiv \langle a^\dagger(t)a(t-\tau)\rangle = \bar{n}\,e^{-\kappa\tau}. \end{aligned} \tag{A7}$$

On using (A4) and (A5), Eq. (A6) reduces to

$$\frac{d\tilde{\rho}_a(t)}{dt} = -g^2(1+\overline{n})\int_0^\infty d\tau\, e^{-\kappa\tau}\left\{G(t)G^\dagger(t-\tau)\,\tilde{\rho}_a(t)\,e^{-i\delta\tau} - G^\dagger(t-\tau)\,\tilde{\rho}_a(t)\,G(t)\,e^{-i\delta\tau} + \text{H.c.}\right\}$$
$$- g^2\,\overline{n}\int_0^\infty d\tau\, e^{-\kappa\tau}\left\{\tilde{\rho}_a(t)\,e^{-i\delta\tau}G^\dagger(t-\tau)G(t) - e^{-i\delta\tau}G(t)\,\tilde{\rho}_a(t)\,G^\dagger(t-\tau) + \text{H.c.}\right\}. \tag{A8}$$

Transforming (A8) to the original picture

$$\begin{aligned}\rho_a(t) &= e^{-iH_at/\hbar}\,\tilde{\rho}_a(t)\,e^{iH_at/\hbar}\,,\\ G(t) &= e^{iH_at/\hbar}\left[2\cos(\theta)\,\sin(\theta)\,R^z + \cos^2(\theta)\,R^+ - \sin^2(\theta)\,R^-\right]e^{-iH_at/\hbar}\\ &= e^{iH_at/\hbar}\,S^+\,e^{-iH_at/\hbar},\end{aligned} \tag{A9}$$

we obtain the density matrix equation for the atom

$$\begin{aligned}\frac{d\rho_a(t)}{dt} &= -\tfrac{i}{\hbar}\left[H_a(t),\rho_a(t)\right]\\ &\quad -g^2(1+\overline{n})\textstyle\int_0^\infty d\tau\,\left\{e^{-\kappa\tau-i\delta\tau}\left[G(0)G^\dagger(-\tau)\,\rho_a(t) - G^\dagger(-\tau)\,\rho_a(t)\,G(0)\right] + \text{H.c.}\right\}\\ &\quad -g^2\,\overline{n}\textstyle\int_0^\infty d\tau\,\left\{e^{-\kappa\tau-i\delta\tau}\left[\rho_a(t)G^\dagger(-\tau)G(0) - G(0)\,\rho_a(t)\,G^\dagger(-\tau)\right] + \text{H.c.}\right\}.\end{aligned} \tag{A10}$$

Substituting (A9) in (A10), we get the final master equation for the reduced density matrix of the atom driven by an external field and interacting with the cavity field at finite temperatures. The cavity field has been treated as a quantized field. From (A10) mean values for the atomic operators $R^\pm$ and R^z can be obtained. Detailed calculations show that they satisfy Eqs. (2.23) in Sec. II. It should be noted that the time dependence of G is determined from the dynamics of the atom in the absence of the cavity field but in the presence of the external field.

The conditions for the validity of Eq. (A10) can be obtained by requiring that the time scale of the terms under the integral in Eq. (A10) is much smaller than the time scales of interest. The time scales appearing under the integral are the inverse generalized Rabi frequency $\overline{\Omega}^{-1}$ associated with $G(t)$ and $(\kappa^2+\delta^2)^{-1/2}$. The time scales of interest were determined in Sec. III and are essentially $\Gamma_\parallel^{-1}$ and $\Gamma_\perp^{-1}$.

APPENDIX B: MODIFIED BLOCH EQUATIONS

For completeness we present the modified Bloch equations in the bare state atomic basis. These can be obtained from (A10). The operator $G(\tau)$ is defined by (A9). We write it as

$$S^+(-\tau) \equiv m_1(\tau)S^+ + m_2(\tau)S^- + m_3(\tau)S^z. \tag{B1}$$

The Laplace transforms of m_1, m_2, and m_3 are found to be

$$\begin{aligned}\hat{m}_1(z) &= \frac{|\Omega|^2 + 2z(z-i\Delta)}{2q(z)}\,,\\ \hat{m}_2(z) &= \frac{\Omega^{*2}}{2q(z)},\\ \hat{m}_3(z) &= \frac{i\Omega^*(z-i\Delta)}{q(z)},\\ q(z) &= z\left(|\Omega|^2 + z^2 + \Delta^2\right),\end{aligned} \tag{B2}$$

where Ω is given by Eq. (2.7). We substitute (B1) in (A10) and take the expectation values. We then obtain the equations

$$\langle\dot{S}^+\rangle = i\Delta\langle S^+\rangle - i\Omega^*\langle S^z\rangle - 2g^2\overline{n}\left\{\hat{m}_1(\kappa-i\delta)\langle S^+\rangle - \hat{m}_2(\kappa-i\delta)\langle S^-\rangle\right\}$$
$$-g^2\left\{\hat{m}_1(\kappa-i\delta)\langle S^+\rangle - \hat{m}_2(\kappa-i\delta)\langle S^-\rangle - \frac{1}{2}\hat{m}_3(\kappa-i\delta)\right\}, \tag{B3a}$$

$$\langle\dot{S}^z\rangle = -\frac{i}{2}\Omega\langle S^+\rangle - g^2\left\{\hat{m}_1(\kappa-i\delta)\left(\frac{1}{2}+\langle S^z\rangle\right) - \frac{1}{2}\hat{m}_3(\kappa-i\delta)\langle S^-\rangle\right\}$$
$$-2g^2\overline{n}\left\{\hat{m}_1(\kappa-i\delta)\langle S^z\rangle - \frac{1}{2}\hat{m}_3(\kappa-i\delta)\langle S^-\rangle\right\} + \text{c.c.} \tag{B3b}$$

These are the modified Bloch equations. In the absence of (or for a weak) driving field we have

$$\begin{aligned} m_1(\tau) &\to e^{-i\Delta\tau}, \quad m_2(\tau) \to 0, \quad m_3(\tau) \to 0\ , \\ \hat{m}_1(z) &\to \frac{1}{z+i\Delta}, \quad \hat{m}_2(z) \to 0, \quad \hat{m}_3(z) \to 0\ , \end{aligned} \tag{B4}$$

and hence Eqs. (B3) reduce to the standard Bloch equations

$$\langle \dot{S}^+ \rangle = i\Delta \langle S^+ \rangle - i\Omega^* \langle S^z \rangle - \frac{g^2(2\overline{n}+1)}{\kappa - i\delta + i\Delta} \langle S^+ \rangle\ , \tag{B5a}$$

$$\langle \dot{S}^z \rangle = -\frac{i}{2}\Omega \langle S^+ \rangle - \frac{g^2}{\kappa - i\delta + i\Delta}\left(\frac{1}{2} + \langle S^z \rangle (2\overline{n}+1)\right) + \text{c.c.} \tag{B5b}$$

The decay rates $\Gamma_\parallel$, $\Gamma_\perp$ and the shift of the generalized Rabi frequency $\Delta\overline{\Omega}$ can also be expressed by the Laplace transforms (B2):

$$\Gamma_\parallel = g^2 \frac{1+2\overline{n}}{\overline{\Omega}^2}\left[(\overline{\Omega}^2 + \Delta^2)\,\mathrm{Re}\{\hat{m}_1(z)\} - \Omega^2\,\mathrm{Re}\{\hat{m}_2(z)\} - \Omega\Delta \mathrm{Re}\{\hat{m}_3(z)\}\right]\ , \tag{B6a}$$

$$\Gamma_\perp = g^2 \frac{1+2\overline{n}}{2\overline{\Omega}^2}\left[(2\overline{\Omega}^2 + \Omega^2)\,\mathrm{Re}\{\hat{m}_1(z)\} + \Omega^2\,\mathrm{Re}\{\hat{m}_2(z)\} + \Omega\Delta\,\mathrm{Re}\{\hat{m}_3(z)\}\right]\ , \tag{B6b}$$

$$\Delta\overline{\Omega} = g^2 \frac{1+2\overline{n}}{2\overline{\Omega}}\left[\Omega\,\mathrm{Im}\{\hat{m}_3(z)\} - 2\Delta\,\mathrm{Im}\{\hat{m}_1(z)\}\right]\ , \tag{B6c}$$

$$z = \kappa - i\delta\ .$$

For numerical computations either Eqs. (B3) or (2.23) can be used. However, the physics is more transparent in the dressed atom picture we have employed to interpret the atomic dynamics in the cavity.

APPENDIX C: SOLUTION OF THE BLOCH EQUATIONS FOR NONADIABATIC PASSAGE

Equations (3.6) derived in Sec. III describe the Bloch vector motion only in cases when the rate of change τ of the coupling constant $g(t)$ is slow compared to other characteristic time scales of the system. This condition is no longer fulfilled, if we want to describe the turn on and turn off of the coupling $g(t)$ in the rest frame of the atoms for detunings $\Delta < \tau^{-1}$ [22].

Here we would like to present a solution, which is valid for arbitrary detunings. We proceed in three steps. First we treat the turn on phase, making use of an analytical solution of the Schrödinger equation for a particular shape of the leading edge of the coupling. We neglect atomic decay during this phase. In the second step we let the Bloch vector of the system evolve according to Eqs. (3.6), as within the cavity the coupling stays constant. Finally, we determine the state of the atom leaving the cavity by inverting the first step.

The particular time dependence of the coupling, and hence of the intracavity Rabi frequency that actually permits an analytical solution to the problem, is [23,24]

$$\Omega(t) = \begin{cases} \Omega_0 & \text{if } |t| \le \frac{T}{2} \\ \Omega_0\ \operatorname{sech}\frac{\pi}{\tau}(|t| - \frac{T}{2}) & \text{if } |t| > \frac{T}{2}, \end{cases} \tag{C1}$$

where Ω_0 is given by the modulus of Eq. (2.7). We start from the Hamiltonian of the system in a frame rotating at the atomic transition frequency ω_0:

$$H = \frac{\hbar}{2}\Omega(t)\left(e^{i\Delta t}S^+ + e^{-i\Delta t}S^-\right). \tag{C2}$$

Introducing the upper and lower level amplitudes $s(t)$ and $p(t)$, the Schrödinger equation obtained from (C2) can be written as

$$\begin{aligned} \dot{p}(t) &= -\frac{i}{2}\,\Omega(t)\,s(t)\,e^{-i\Delta t}\ , \\ \dot{s}(t) &= -\frac{i}{2}\,\Omega(t)\,p(t)\,e^{i\Delta t}. \end{aligned} \tag{C3}$$

We now shift the time origin by $-T/2$, absorb the additional phase factor $e^{-i\Delta T/2}$ in s, and transform the time t to a new variable z defined by

$$z = \frac{1}{2}\left[\tanh\frac{\pi t}{\tau} + 1\right]. \tag{C4}$$

Then the Schrödinger equation assumes the form

$$\begin{aligned} p'(z) &= -ia\frac{1}{z}\left(\frac{1}{z}-1\right)^{-\Phi} s(z)\ , \\ s'(z) &= -ia\frac{1}{z}\left(\frac{1}{z}-1\right)^{-\Phi^*} p(z), \end{aligned} \tag{C5}$$

where

$$a = \left|\frac{\Omega_0\tau}{2\pi}\right|\ , \quad \Phi = \frac{1}{2} - i\frac{\Delta\tau}{2\pi}. \tag{C6}$$

Equations (C5) can be transformed to a hypergeometric equation for p(z):

$$z(1-z)p''(z) + (1-z-\Phi)p'(z) + a^2 p(z) = 0. \tag{C7}$$

Its solutions are the hypergeometric functions

$$\begin{aligned} f_1(z) &= F(a,-a;1-\Phi;z)\ , \\ f_2(z) &= \frac{a}{\Phi}\,z^\Phi\,F(\Phi+a,\Phi-a;1+\Phi;z), \end{aligned} \tag{C8}$$

which are normalized such that $|f_1|^2+|f_2|^2 = 1$. Inserting into Eqs. (C5) we obtain the general solution for the level amplitudes during the leading edge of the cavity mode:

$$\begin{aligned} p(z) &= \alpha\, f_1(z) + \beta\, f_2(z)\ , \\ s(z) &= -i\alpha\, f_2^*(z) + i\beta f_1^*(z), \end{aligned} \tag{C9}$$

TABLE I. Special values of the hypergeometric functions appearing in the solution (C8) of the Schrödinger equation for a two-level atom irradiated by a hyperbolic secant pulse.

z	$f_1(z)$	$f_2(z)$
0	1	0
0.5	$f_0^*(\Phi,a)+f_0^*(\Phi,-a)$	$f_0(\Phi,a)-f_0(\Phi,-a)$
1	$\dfrac{\Gamma^2(1-\Phi)}{\Gamma(1-\Phi-a)\Gamma(1-\Phi+a)}$	$\dfrac{\sin\pi a}{\sin\pi\Phi}$

with $f_0(\Phi,a)=\dfrac{\sqrt{\pi}}{2^\Phi}\dfrac{\Gamma(\Phi)}{\Gamma\left(\frac{\Phi+a}{2}\right)\Gamma\left(\frac{\Phi-a+1}{2}\right)}$

where the condition $|\alpha|^2+|\beta|^2=1$ must hold to ensure the correct normalization. From α and β expectation values of the spin operators can be calculated using

$$\langle S^+\rangle = s^* p\, e^{i\Delta t}\ ,\quad \langle S^z\rangle = \frac{1}{2}\left(|s|^2-|p|^2\right)\ , \tag{C10}$$

and the matrix

$$A(z)=\begin{pmatrix} \frac{1}{2}\left(|f_2|^2-|f_1|^2\right) & -f_1 f_2^* & -f_1^* f_2 \\ i f_1 f_2 & -i f_1^2 & i f_2^2 \\ -i f_1^* f_2^* & -i(f_2^*)^2 & i(f_1^*)^2 \end{pmatrix}. \tag{C11}$$

We obtain the matrix equation

$$\begin{pmatrix} \langle S^z\rangle \\ \langle S^+\rangle \\ \langle S^-\rangle \end{pmatrix} = A(z) \begin{pmatrix} |\alpha|^2-|\beta|^2 \\ \alpha\beta^* e^{i\Delta t} \\ \alpha^*\beta e^{-i\Delta t} \end{pmatrix}. \tag{C12}$$

The parameters α and β are determined by the initial conditions at $t\to-\infty$ ($z=0$), up to a phase factor, and are constant in time. Therefore, we can obtain the Bloch vector at an arbitrary time z during the turn on of the coupling, by multiplying the initial Bloch vector by the matrix $A(z)A^{-1}(0)$, using Eq. (C12) and its inverse. Finally, we transform to the dressed picture by multiplying with the matrix

$$B(\theta)=\begin{pmatrix} \cos 2\theta & \frac{1}{2}\sin 2\theta & \frac{1}{2}\sin 2\theta \\ -\sin 2\theta & \cos^2\theta & -\sin^2\theta \\ -\sin 2\theta & -\sin^2\theta & \cos^2\theta \end{pmatrix}, \tag{C13}$$

where the mixing angle θ is defined in (2.15)

Thus we are able to determine the Bloch vector at the end of the turn on phase ($z=0.5$). Starting with an atom in the upper state ($\langle S^z\rangle = 1/2$, $\langle S^\pm\rangle = 0$), we obtain

$$\begin{pmatrix} \langle R^z\rangle \\ \langle R^+\rangle \\ \langle R^-\rangle \end{pmatrix}_{-T/2} = B(\theta)\, A(0.5)\, A^{-1}(0) \begin{pmatrix} 1/2 \\ 0 \\ 0 \end{pmatrix}. \tag{C14}$$

Expression (C14) is the initial condition for Eqs. (3.6). As a reasonable approximation we set $\langle R^+(t)\rangle$ in Eq. (3.6a), rapidly oscillating at the frequency $\tilde{\Omega}$, equal to zero, as for a strong driving field the oscillations are washed out if the distribution of transit times has a width larger than $\tilde{\Omega}^{-1}$. Therefore, we only have to use Eq. (3.6b) to obtain $\langle R^z\rangle$ at time $T/2$, when the coupling starts to decrease. The Bloch vector at the detector, i.e., at time $t\to\infty$ ($z=1$), can then be calculated by inverting the steps that have led to Eq. (C14):

$$\begin{pmatrix} \langle S^z\rangle \\ \langle S^+\rangle \\ \langle S^-\rangle \end{pmatrix}_{\infty} = A(1)\, A^{-1}(0.5)\, B(-\theta) \begin{pmatrix} \langle R^z\rangle \\ 0 \\ 0 \end{pmatrix}_{T/2}. \tag{C15}$$

In (C14) and (C15) we have to evaluate the matrix $A(z)$ at the three values $z=0$, 0.5, and 1. At these points the functions f_1 and f_2 appearing in A can be expressed by elementary functions, which have been compiled in Table I. The final expression for the inversion of the atoms leaving the cavity, in the bare state basis, is

$$\begin{aligned}
\langle S^z\rangle_{\text{final}} = {} & \left(2\sin(2\theta)\,\mathrm{Im}\{f_2^*(1)f_1(1)[f_1^{*2}(0.5)+f_2^2(0.5)]\}\right. \\
& +2\sin(2\theta)\,\mathrm{Im}\{f_1(0.5)\,f_2(0.5)\}[|f_1(1)|^2-|f_2(1)|^2] \\
& +4\cos(2\theta)\,\mathrm{Re}\{f_2(0.5)\,f_1(1)\,f_1^*(0.5)\,f_2^*(1)\} \\
& \left.+\cos(2\theta)[|f_1(0.5)|^2-|f_2(0.5)|^2][|f_1(1)|^2-|f_2(1)|^2]\right)\frac{\Gamma_+-\Gamma_-}{2\Gamma_\parallel}\left[\exp(-\Gamma_\parallel T)-1\right] \\
& +[(2-3\sin^2 2\theta)\,\mathrm{Re}\{f_2(0.5)\,f_1(1)\,f_1^*(0.5)\,f_2^*(1)\}[|f_1(0.5)|^2-|f_2(0.5)|^2] \\
& -(2-3\sin^2 2\theta)\,[|f_1(1)|^2-|f_2(1)|^2]|f_1(0.5)|^2|f_2(0.5)|^2 \\
& +2\sin(2\theta)\cos(2\theta)[|f_1(1)|^2-|f_2(1)|^2]\mathrm{Im}\{f_1(0.5)\,f_2(0.5)\}\,[|f_1(0.5)|^2-|f_2(0.5)|^2]
\end{aligned}$$

$$
\begin{aligned}
&+\sin(2\theta)\cos(2\theta)\mathrm{Im}(f_2^*(1)\,f_1(1)\{[3-4\,|f_2(0.5)|^2]f_2^2(0.5)+[1-4\,|f_2(0.5)|^2]f_1^{*2}(0.5)\}) \\
&+0.5\cos^2(2\theta)[|f_1(1)|^2-|f_2(1)|^2] \\
&+\sin^2(2\theta)\mathrm{Re}\{(f_2^*(1)\,f_1(1)\,[f_1^{*3}(0.5)\,f_2^*(0.5)-f_1(0.5)\,f_2^3(0.5)]\} \\
&-\sin^2(2\theta)[\,|f_1(1)|^2-|f_2(1)|^2]\mathrm{Re}\left\{f_1^2(0.5)f_2^2(0.5)\right\}]\exp(-\Gamma_{\|}T). \qquad \text{(C16)}
\end{aligned}
$$

In the limit of large detuning of the driving field, expression (C16) reduces to the adiabatic result (4.2). If the detuning is of the order of κ or smaller, (C16) cannot be simplified any further. Therefore, in Sec. IV we have evaluated the expression numerically.

[1] E. M. Purcell, Phys. Rev. **69**, 681 (1946).

[2] P. Goy, J. M. Raimond, M. Gross, and S. Haroche, Phys. Rev. Lett. **50**, 1903 (1983).

[3] Y. Kaluzny *et al.*, Phys. Rev. Lett. **51**, 1175 (1983).

[4] G. S. Agarwal, in *Quantum Electrodynamics and Quantum Optics*, edited by A. O. Barut (Plenum, New York, 1984), p. 1.

[5] D. Kleppner, Phys. Rev. Lett. **47**, 233 (1981); R. G. Hulet, E. S. Hilfer, and D. Kleppner, *ibid.* **55**, 2137 (1985).

[6] S. Haroche and J. M. Raimond, in *Advances in Atomic and Molecular Physics*, edited by D. R. Bates and B. Bederson (Academic, New York, 1985), Vol. 20, p. 347.

[7] J. A. Gallas, G. Leuchs, and H. Walther, in *Advances in Atomic and Molecular Physics* (Ref. [6]), p. 413.

[8] For cavity modified decay rates at optical frequencies see D. J. Heinzen, J. J. Childs, J. E. Thomas, and M. S. Feld, Phys. Rev. Lett. **58**, 1320 (1987).

[9] Lewenstein *et al.* consider atomic decay in the presence of a color reservoir. They use modified Bloch equations in non-Markovian form and show how the effects of a color reservoir can be inhibited at large driving fields. M. Lewenstein, T. W. Mossberg, and R. J. Glauber, Phys. Rev. Lett. **59**, 775 (1987); M. Lewenstein, J. Zakrezewski, and T. W. Mossberg, Phys. Rev. A **38**, 808 (1988).

[10] B. R. Mollow, Phys. Rev. **188**, 1969 (1969).

[11] W. Lange and H. Walther, Phys. Rev. A **48**, 4551 (1993).

[12] Y. Zhu, A. Lezama, M. Lewenstein, and T. W. Mossberg, Phys. Rev. Lett. **61**, 1946 (1988).

[13] B. R. Mollow, Phys. Rev. A **12**, 1919 (1975).

[14] R. J. Glauber, Phys. Rev. **131**, 2766 (1963).

[15] G. S. Agarwal, *Quantum Optics*, edited by G. Höhler, Springer Tracts in Modern Physics Vol. 70 (Springer, Berlin, 1974), Sec. VI.

[16] A first-principle derivation of this is given in R. K. Bullough, Hyperfine Interact. **37**, 71 (1987), Appendix.

[17] D. P. O'Brien, P. Meystre, and H. Walther, Adv. At. Mol. Phys. **21**, 1 (1985).

[18] W. Jhe *et al.*, Phys. Rev. Lett. **58**, 666 (1987).

[19] Semiclassical dressed states have been used extensively in understanding the fluorescence and absorption spectra of radiating atoms in free space, see, for example, G. S. Agarwal, Phys. Rev. A **19**, 923 (1979); Y. S. Bai, A. G. Yodh, and T. W. Mossberg, Phys. Rev. Lett. **55**, 1277 (1985).

[20] For dressed states of the atom interacting with a quantized radiation field, see C. Cohen-Tannoudji, J. Dupont-Ruc, and G. Grynberg, *Atom-Photon Interactions—Basic Processes and Applications* (Wiley, New York, 1992), Chap. VI.

[21] The modification of Mollow spectra by the cavity field in the optical domain has been reported by Y. Zhu, A. Lezama, and T. W. Mossberg, Phys. Rev. A **39**, 2268 (1989); for the corresponding theoretical developments see D. Holm, M. Sargent III, and S. Stenholm, J. Opt. Soc. Am. B **2**, 1456 (1985); G. S. Agarwal, Phys. Rev. A **42**, 2886 (1990).

[22] E. Courtens and A. Szöke, Phys. Rev. A **15**, 1588 (1977).

[23] N. Rosen and C. Zener, Phys. Rev. **40**, 502 (1932).

[24] R. T. Robiscoe, Phys. Rev. A **17**, 247 (1978).